DOI: 10.1002/chem.200601406

The Complete Structure and Pro-inflammatory Activity of the Lipooligosaccharide of the Highly Epidemic and Virulent Gram-Negative Bacterium *Burkholderia cenocepacia* ET-12 (Strain J2315)

Alba Silipo,[a] Antonio Molinaro,*[a] Teresa Ieranò,[a] Anthony De Soyza,[b] Luisa Sturiale,[c] Domenico Garozzo,[c] Christine Aldridge,[d] Paul A. Corris,[b] C. M. Anjam Khan,[d] Rosa Lanzetta,[a] and Michelangelo Parrilli[a]

Abstract: Members of genus *Burkholderia* include opportunistic Gram-negative bacteria that are responsible for serious infections in immunocompromised and cystic fibrosis (CF) patients. The *Burkholderia cepacia* complex is a group of microorganisms composed of at least nine closely related genomovars. Among these, *B. cenocepacia* is widely recognized to cause epidemics associated with excessive mortality. Species that belong to this strain are problematic CF pathogens because of their high resistance to antibiotics, which makes respiratory infections difficult to treat and impossible to eradicate. Infection by these bacteria is associated with higher mortality in CF and poor outcomes following lung transplantation. One virulence factor contributing to this is the pro-inflammatory lipopolysaccharide (LPS) molecules. Thus, the knowledge of the lipopolysaccharide structure is an essential prerequisite to the understanding of the molecular mechanisms involved in the inflammatory process. Such data are instrumental in aiding the design of antimicrobial compounds and for developing therapeutic strategies against the inflammatory cascade. In particular, defining the structure of the LPS from *B. cenocepacia* ET-12 clone LMG 16656 (also known as J2315) is extremely important given the recent completion of the sequencing project at the Sanger Centre using this specific strain. In this paper we address this issue by defining the pro-inflammatory activity of the pure lipopolysaccharide, and by describing its full primary structure. The activity of the lipopolysaccharide was tested as a stimulant in human myelomonocytic U937 cells. The structural analysis was carried out by compositional analysis, mass spectrometry and 2D NMR spectroscopy on the intact lipooligosacchride (LOS) and its fragments, which were obtained by selective chemical degradations.

Keywords: *Burkholderia cenocepacia* ET-12 · cystic fibrosis · lipooligosaccharides · mass spectrometry · NMR spectroscopy

Introduction

In this paper we show that the high pro-inflammatory activity of *B. cenocepacia* ET-12 type strain LMG 16656 is due to the lipopolysaccharide (LPS), and we carry out a detailed chemical study on its LPS structure by means of chemical analyses, matrix-assisted laser desorption/ionization mass spectrometry and 2D NMR spectroscopy.

[a] Dr. A. Silipo, Prof. A. Molinaro, Dr. T. Ieranò, Prof. R. Lanzetta, Prof. M. Parrilli
Dipartimento di Chimica Organica e Biochimica
Università di Napoli, Complesso Universitario Monte Sant'angelo
Via Cintia 4, 80126 Napoli (Italy)
Fax: (+39) 081-674-393
E-mail: molinaro@unina.it

[b] Dr. A. De Soyza, Prof. P. A. Corris
Transplantation and Immunobiology Group
The Freeman Hospital, High Heaton
Newcastle upon Tyne NE7 7DN (UK)

[c] Dr. L. Sturiale, Dr. D. Garozzo
Istituto per la Chimica e la Tecnologia dei Materiali Polimerici
ICTMP-CNR, Catania (Italy)

[d] C. Aldridge, Prof. C. M. A. Khan
Institute for Cell and Molecular Biosciences
The Medical School, University of Newcastle
Newcastle (UK)

Supporting information for this article is available on the WWW under http://www.chemeurj.org/ or from the author. It contains the SDS-gel electrophoretic comparison of LPS from *Burkholderia cenocepacia* ET-12 clones and *Burkholderia multivorans* strain LMG 14273 (in Figure S1); monosaccharide components of **LOS**, **OS1**, **OS2** and **OS3** in Table S1; comparison of ^{1}H NMR spectra of **OS1** and **OS2** products; and structural characterization of the de-O-acylated LOS fraction (with Figure S3 and Table S2).

The genus *Burkholderia*[1–4] comprises more than 30 species, which include animal and plant pathogens, as well as environmental bacteria that inhabit diverse ecological niches and have been isolated from soil, water, plants, insects, industrial settings, hospital environments and from infected humans.[1] Several *Burkholderia* strains have attracted considerable interest from the biotechnological and agricultural industry for bioremediation of recalcitrant xenobiotics, plant growth promotion and biocontrol purposes. *Burkholderia* species have emerged as problematic opportunistic pathogens in cystic fibrosis (CF) patients and in immunocompromised individuals.[1–4] These species comprise a heterogeneous group of genetically distinct strains, each known as a genomovar. The *B. cepacia* complex (BCC)[2] consists of nine described species that share a high degree of 16S rDNA sequence similarity (98–100%), and only moderate levels of DNA–DNA hybridization: *B. cepacia*, *B. multivorans*, *B. cenocepacia*, *B. stabilis*, *B. vietnamiensis*, *B. dolosa*, *B. ambifaria*, *B. anthina* and *B. pyrrocinia*. BCC strains can cause life-threatening lung infections in individuals with chronic granulomatous disease, or with CF. Species that belong to the BCC are problematic CF pathogens because of their high resistance to antibiotics, which makes respiratory infection difficult to treat and impossible to eradicate. Infection by these bacteria is associated with higher mortality in CF and poorer outcomes following lung transplantation compared to those patients with pretransplant *Pseudomonas aeruginosa* infections. Many species are highly epidemic and spread easily within CF centres from one patient to another, which leads to considerable anxiety and segregation policies.

The majority of BCC species that have been isolated from cystic fibrosis centres belong to *B. multivorans* (BCC genomovar II) and *B. cenocepacia* (BCC genomovar III).[3–4] *B. cenocepacia* accounts for the majority of isolates. Within this grouping, there are a number of strains that are responsible for causing often fatal epidemics, in particular the ET-12 clone. The ET-12 strain predominates in several CF centres and has enhanced virulence and capacity of spread.[3–4] The higher mortality rates following lung transplantation appear to be restricted to ET-12-infected patients.[5,6] For these reasons, it has been designed as the type strain and its genome has been sequenced at the Sanger Centre.

The pathogenic mechanisms that lead to poor clinical outcomes are only just beginning to be explored at the molecular level. Several virulence factors have been defined for *B. cenocepacia*, one of the most important of which is the lipopolysaccharide (LPS) molecule.[7–10] Lipopolysaccharides are heat-stable, complex amphiphilic macromolecules that are indispensable for the growth and survival of Gram-negative bacteria; they are also called endotoxins because they are cell-bound, and once released, they play a key role in the pathogenesis of Gram-negative infections. LPSs compose about 75% of the outer membrane of Gram-negative bacteria and are exposed to the external environment. They have common structural motifs composed of a hydrophilic heteropolysaccharide (formed by a core oligosaccharide and an O-specific polysaccharide or O-chain) that is covalently linked to a lipophilic moiety termed lipid A, which is embedded in the outer leaflet and anchors these macromolecules to the membrane through electrostatic and hydrophobic interactions. LPSs that do not possess the O-chain are termed rough LPSs (R-LPSs) or lipooligosaccharides (LOSs). LOSs can occur either in wild strains, or in laboratory strains that posess mutations in the genes encoding for either the O-specific polysaccharide biosynthetic enzymes, or for proteins devoted to its transfer through the membrane. Lipid A possesses a rather conservative structure that usually consists of a β-(1→6)-glucosamine disaccharide backbone that is phosphorylated at the 1- and 4′-positions, and is acylated with primary 3-hydroxy fatty acids at the 2- and 3-positions of both GlcN residues. The hydroxyl groups of the primary fatty acids can be further acylated by secondary acyl moieties. In the core oligosaccharide, the inner and outer regions are usually distinguished: the inner core, proximal to the lipid A, consists of typical mannose residues like Kdo (3-deoxy-D-*manno*-oct-2-ulosonic acid) and heptoses. Kdo is the linker between the GlcN II of the lipid A backbone and the inner core portion. The outer core region is more variable and is usually composed of hexoses.[9,10] Surprisingly, few data are available for the LPS structure from *B. cenocepacia* in general, and in particular for the ET-12 clone LMG 16656 (also known as J2315), despite it being the designated type strain that was used for genome sequencing at the Sanger Centre. The elucidation of the LPS structure is an essential prerequisite for the understanding of the molecular mechanisms that are involved in the inflammatory process. Such data are instrumental in aiding the design of antimicrobial compounds and for the development of therapeutic strategies against the inflammatory cascade. Furthermore, the observations of the high pro-inflammatory activity of the ET-12 clone by using LPS-rich whole-cell lysates as stimulants in human myelomonocytic U937 cells[5] prompted us to start the isolation of the pure LPS molecules in order to test their activity and to determine the structure as the first step toward a structure–activity comparison between the *B. cenocepacia* ET-12 clones relative to the other LPS from the *B. cepacia* complex.

Results

SDS electrophoresis analysis and biological activity of ET-12 LPSs: A LPS fraction was extracted from *B. cenocepacia* ET-12 strains LMG 16656, the type strain recently sequenced at the Sanger Centre, from strain LMG 18863 (also known as k56-2, an ET-12 clone) and from strain LMG 12614, and eventually, a LPS from the clinically derived *B. multivorans* strain LMG 14273. These fractions were analyzed by SDS electrophoresis; LMG 12614, LMG 16656 and LMG 14273 were found to run to the bottom of the gel, which is typical for R-type LPS (LOS), whereas LGM 18863 behaved like a typical S-LPS (Figure S1 available in the Supporting Information).

The three *B. cenocepacia* ET-12 LOSs were tested and compared with *B. multivorans* LOS for their pro-inflammatory activity, in particular, for TNF-α induction in human myelomonocytic U937 cells. We found that the type strain *B. cenocepacia* ET-12 LMG 16656 was capable of inducing significantly greater levels of TNF-α induction relative to *B. multivorans* LMG 14273 ($p < 0.05$) and in general, all ET-12 strains induced significantly more TNF-α induction than the *B. multivorans*, even though there were significant differences in cytokine induction (Figure 1). These data are consistent with our prior observations from using LPS-rich whole cell lysates as stimulants in the same reporter assay.[5]

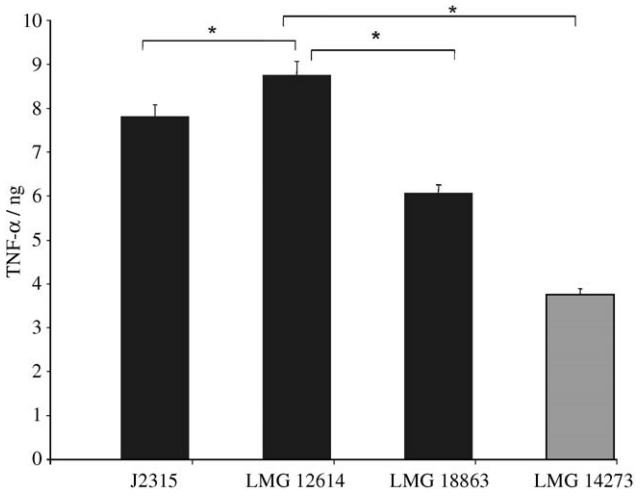

Figure 1. A comparison of the ability of purified LPS from *Burkholderia* species to induce TNF-α production in a U937 macrophage reporter assay. Purified LPS (100 ng) from three ET-12 *B. cenocepacia* clones (solid bars) and *B. multivorans* strain LMG 14273 were incubated with differentiated U937 macrophages for 24 h. The resultant supernatants were assayed for tumour necrosis factor-alpha (TNF-α) activity by ELISA. Significantly higher TNF-α was elicited by any of the ET-12 clones ($p < 0.05$) as compared to the *B. multivorans*.

Isolation and compositional analysis of LOS, OS1 and OS2 from *B. cenocepacia* ET-12 strains LMG 16656: The isolated LPS from LMG 16656 was a rough chemotype (LOS), as suggested by SDS-PAGE (Figure S1 available in the Supporting Information) and was subjected to a full structural investigation.

Monosaccharide analyses of the isolated LOS from LMG 16656 revealed the presence of L-Rha, 2,6-dideoxy-2-amino-D-glucose (D-quinovosamine, D-QuiN), D-GlcN, 4-amino-4-deoxy-L-arabinose (L-Ara4N), D-Glc, D-Gal, L-*glycero*-D-*manno*-heptose (L,D-Hep), 3-deoxy-D-*manno*-oct-2-ulopyranosonic acid (D-Kdo) and D-*glycero*-D-*talo*-oct-2-ulopyranosonic acid (D-Ko). Methylation analysis revealed the presence of 3,4-disubstituted Hep, 3,7-disubstituted Hep, 7-substituted Hep, terminal Hep, 2,6-disubstituted Gal, 6-substituted Glc, terminal Glc, terminal Rha, terminal Ara4N, 6-substituted GlcN, 3-substituted QuiN, 4,5-disubstituted Kdo, 8-substituted Ko and terminal Ko, all as pyranose rings and with a high GLC retention time of a heptose disaccharide formed by Hep-(1→7)-Hep. In agreement with the published method,[11] a mild methanolysis on the intact LOS (0.5 M HCl/MeOH, 85 °C, 45 min) allowed the isolation of the trisaccharide formed by Ara4N-(1→8)-Ko-(2→4)-Kdo.

A fatty acids analysis revealed the presence of (*R*)-3-hydroxyhexadecanoic (C16:0 (3-OH)) in an amide linkage and (*R*)-3-hydroxytetradecanoic (C14:0 (3-OH)) acid and tetradecanoic acid (C14:0) in ester linkages.

To determine the primary structure of the core portion of *B. cenocepacia*, a mild hydrolysis with acetate buffer was performed in order to cleave lipid A from the core oligosaccharide fraction. After gel-permeation chromatography, two fractions, **OS1** and **OS2** were isolated.

The compositional analysis (Table S1 available in the Supporting Information) of the isolated **OS1** revealed the presence of L-Rha, D-QuiN, D-Glc, D-Gal, L,D-Hep, D-Kdo. Methylation analyses showed the presence of a 3,4-disubstituted Hep, a 3,7-disubstituted Hep, a terminal Hep, a 2,6-disubstituted Gal, a terminal Glc, a terminal Rha, a 3-substituted QuiN, a 5-substituted Kdo and a small amount of 6-substituted Glc, all in the pyranose ring form.

The compositional analysis of the isolated **OS2** showed an additional D-Ko residue, whereas the linkage analysis showed the additional presence of a 4,5-disubstituted Kdo, a terminal Ko and a 7-substituted Hep with respect to **OS1**, and of a heptose disaccharide formed by Hep-(1→7)-Hep. A mild methanolysis treatment (0.5 M HCl/MeOH, 85 °C, 45 min) allowed the isolation of the disaccharide formed by Ko-(2→4)-Kdo.[11]

Structural characterisation of the OS1 product: The ^{1}H NMR spectra of **OS1** and **OS2** are shown in Figure S2. A combination of homo- and heteronuclear 2D NMR experiments (DQF-COSY, TOCSY, ROESY, ^{1}H–^{13}C HSQC and ^{1}H–^{13}C HMBC) was executed in order to assign all of the spin systems of **OS1** and the monosaccharide sequence. In the anomeric region of the ^{1}H NMR spectrum (Figure 2), ten anomeric signals were identified (**A**–**I**, Table 1); furthermore, the signals at $\delta = 1.86/2.16$ ppm were identified as the H-3 methylene of the Kdo residue. The anomeric configuration of each monosaccharide unit was assigned on the basis of the $^3J_{H1,H2}$ coupling constants that were obtained from the DQF-COSY spectrum and the intraresidual NOE contacts that were observed in the ROESY spectrum; the values of the vicinal $^3J_{H,H}$ coupling constants allowed the identification of the relative configuration of each residue. The proton resonances of all spin systems were obtained by DQF-COSY and TOCSY spectra (Figure 3) and were used to assign the carbon resonances in the HSQC spectrum. The NMR data indicated the existence of a mixture of two oligosaccharides with different carbohydrate chain lengths.

Spin system **A**, H-1 at 5.47 ppm (Figure 2, Table 1) was identified as α-galactose, as indicated by its low $^3J_{H3,H4}$ and $^3J_{H4,H5}$ values (3 Hz and 1 Hz, respectively), which are diagnostic of an α-*galacto*-configuration. The H-1 and C-1 chem-

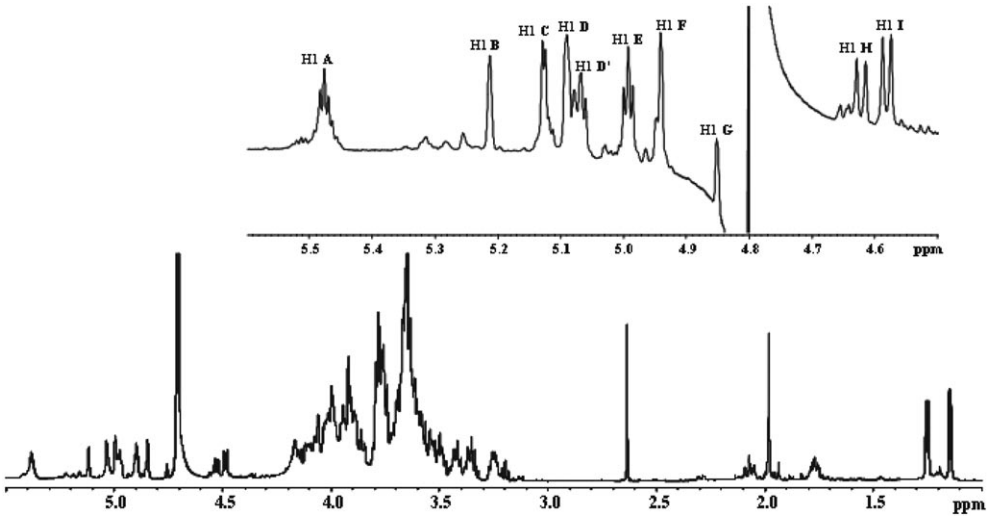

Figure 2. ^{1}H NMR spectrum of **OS1** product. In the inset the expanded anomeric region is shown. Anomeric signals of spin system are designated as in Table 1.

Table 1. ^{1}H and ^{13}C (*italic*) NMR chemical shifts [ppm] of sugar residues of the core lipid A region of the oligosaccharide **OS**. The heptose residues possess a L-*glycero*-D-*manno* configuration, both rhamnose and quinovosamine residues posess a L-configuration, while the other residues posess a D-configuration.

	Chemical shift δ (^{1}H/^{13}C)							
Unit	1	2	3	4	5	6	7	8
A	5.47	3.69	3.85	4.11	3.85	4.09/3.71		
2,6-α-Gal	*97.4*	*74.6*	*71.4*	*70.9*	*71.4*	*65.1*		
B	5.21	4.26	4.00	3.74	3.66	4.16	3.73	
3,7-α-Hep	*100.9*	*69.3*	*79.7*	*72.6*	*71.1*	*68.1*	*69.6*	
C	5.13	4.09	4.21	4.21	3.75	4.03	3.75	
3,4-α-Hep	*100.7*	*55.8*	*73.1*	*73.1*	*72.9*	*68.8*	*62.9*	
D	5.08	3.99	3.86	3.77	3.74	3.87	4.00/3.81	
7-α-Hep	*101.6*	*70.0*	*70.6*	*72.2*	*72.3*	*70.7*	*72.3*	
D′	5.07	3.99	3.86	3.63	3.74	4.03	3.75	
t-α-Hep	*101.6*	*70.0*	*70.6*	*71.2*	*72.2*	*68.8*	*62.9*	
E	4.99	3.57	3.71	3.44	3.75	3.77/3.85		
t-α-Glc	*97.9*	*71.6*	*71.8*	*71.7*	*73.0*	*60.4*		
F	4.94	4.00	3.87	3.63	3.74	4.03	3.75	
t-α-Hep	*100.3*	*69.9*	*70.6*	*71.2*	*72.2*	*68.8*	*62.9*	
G	4.85	3.79	3.74	3.43	4.02	1.23		
t-α-Rha	*101.4*	*70.8*	*72.2*	*72.0*	*69.7*	*16.1*		
H	4.62	3.84	3.55	3.29	3.52	1.34		
3-β-QuiN	*100.3*	*55.5*	*81.5*	*73.2*	*75.5*	*16.9*		
I	4.58	3.33	3.50	3.45	3.46	3.76/3.95		
t-β-Glc	*102. 3*	*73.7*	*75.7*	*69.5*	*76.4*	*61.4*		
K	–	–	1.86/2.16	4.12	4.15	3.67	3.76	3.86/3.60
5-α-Kdo	*174.4*	*95.3*	*34.1*	*65.8*	*74.3*	*71.3*	*69.1*	*63.4*

ical shifts ($\delta = 5.47$ and 97.47 ppm),the $^{3}J_{H1,H2}$, value and the intraresidual NOE contact of H-1 with H-2 were all in agreement with an α-anomeric configuration and a $^{4}C_{1}$ ring conformation.

Spin systems **B**, **C**, **D**, **D′**, **F** (Table 1), were all identified as α-heptose residues, as indicated by their $^{3}J_{H1,H2}$ and $^{3}J_{H2,H3}$ coupling constants (below 3 Hz), and by the intraresidual NOE of H-1 with H-2. The ^{13}C chemical shift value of C-6 of these heptose residues (all below $\delta = 70$ ppm) allowed us to identify them as L-*glycero*-D-*manno*-heptose, in accordance with the chemical analysis.

Spin systems **E** and **I** (Table 1) were identified as glucose residues, as indicated by their large ring $^{3}J_{H,H}$ coupling constants (above 10 Hz). The strong intraresidue NOE contacts of H-1 **I** with H-3 and H-5 **I**, together with the $^{3}J_{H1,H2}$ coupling constant (7 Hz) was diagnostics of β-configuration of residue **I**, whereas the intraresidue NOE contact of H-1 with H-2, and the $^{3}J_{H1,H2}$ coupling constant (3 Hz) were indicative of an α-anomeric configuration of residue **E**.

Residue **G** (H-1 at $\delta =$ 4.85 ppm) was recognized as a α-rhamnose residue. Actually, in the TOCSY spectrum, scalar correlations of the ring protons with methyl signals in the shielded region at $\delta = 1.23$ ppm were visible. The *manno* configuration of residue **G** was established from the $^{3}J_{H1,H2}$ and $^{3}J_{H1,H2}$ values, the α-configuration was assigned by the intraresidual NOE contact of H-1 with H-2 and by the chemical shift of its H-5 and C-5.

Residue **H** (H-1 at $\delta = 4.62$ ppm) was recognized as a β-quinovosamine (β-QuiN), that is, possessing a *gluco* configuration as indicated by the ring $^{3}J_{H,H}$ coupling constants (above 10 Hz). The intraresidual NOE contact of H-1 with H-3 and H-5, and the $^{3}J_{H1,H2}$ coupling constant were indicative of β-anomeric configuration. The ^{13}C–^{1}H HSQC spectrum showed the correlation of H-2 **H**, at $\delta = 3.84$ ppm, with a nitrogen-bearing carbon signal at $\delta = 55.5$ ppm. The down-

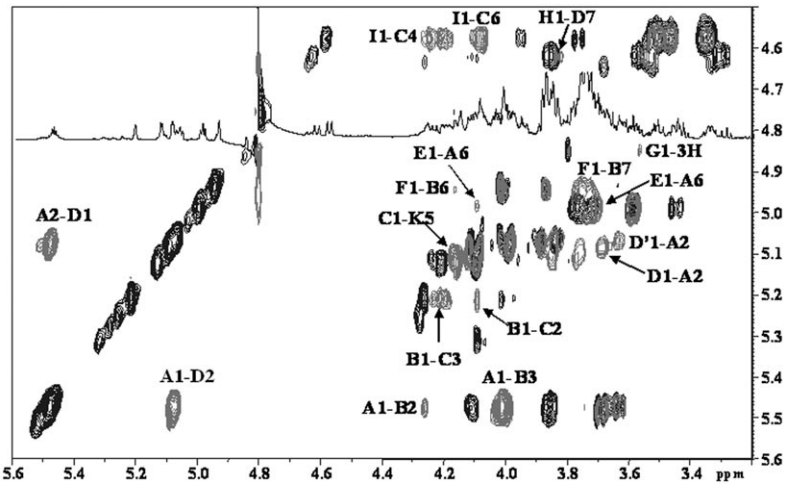

Figure 3. Section of the ROESY (grey) and TOCSY (black) spectrum of oligosaccharide OS1. Monosaccharide labels are as indicated in Table 1. The relevant interresidue ROE crosspeaks are indicated. The presence of a terminal non-stoichiometric disaccharide induces a visible shift in the H-2 A signals.

field shift of proton resonance of H-2 **H** was diagnostic of *N*-acetylation at this position, which was also confirmed by the dipolar correlation of H-2 **H** with the methyl protons of the acetyl group resonating at $\delta = 1.98$ ppm.

Because of the absence of the anomeric proton signal, the spin system of Kdo **K** was assigned starting from the diastereotopic H-3 methylene protons, which resonate in a shielded region at $\delta = 1.86$ and 2.16 ppm (H-3_{ax} and H-3_{eq}, respectively). Because of its free reducing end, the Kdo residue was present in multiple forms. Nevertheless, the signals that belonged to the α-reducing unit were clearly noticeable, and the α-anomeric orientation at C-2 was assigned by the chemical shift values of H-3, and by the values of the $^3J_{H7,H8a}$ and $^3J_{H7,H8b}$ coupling constants.[12,13]

The downfield shift of the carbon resonances identified the glycosylated positions: O-2 and O-6 of residues **A**, O-3 and O-7 of **B**, O-3 and O-4 of **C**, O-7 of **D**, O-3 of **H** and O-5 of **K**, whereas residues **D′**, **E**, **F**, **G**, **I** were non-reducing terminal sugars, in full agreement with the methylation analysis data. The interresidual NOE contacts (Figure 3) and the long-range correlations present in the HMBC spectrum confirmed the oligosaccharide sequence.

The linkage of the heptose **C** to O-5 of Kdo **K** was proven by the downfield shifts of the signal for its C-5 (α-Kdo, $\delta = 74.3$ ppm) and by the NOE connectivity between H-1 of the heptose **C** ($\delta = 5.13$ ppm) and H-5 and H-7 of Kdo ($\delta = 4.15$ and 3.76 ppm, respectively).

Residue **C** was substituted at O-3 and O-4. The NOE contact (Figure 3) of H-4 ($\delta = 4.21$ ppm), H-3 and H-6 **C** with H-1 **I** ($\delta = 4.58$ ppm) evidenced that the O-4 of α-heptose **C** was glycosylated by residue **I**, the β-glucose. Residue **C** was also substituted at O-3 by residue **B**, according to the NOE (Figure 3) of H-3 and H-2 **C** with H-1 **B** ($\delta = 5.21$ ppm). Residue **B** was identified as the 3,7-disubstituted α-heptose. The NOE correlation of H-3 **B** ($\delta = 4.00$ ppm) with H-1 **A** ($\delta = 5.47$ ppm) (Figure 3) gave evidence for the substitution of residue **B** at O-3 by the α-galactose **A**. Furthermore, residue **B** was glycosylated at O-7 by the heptose residue **F**, as demonstrated by the NOE contact of H-7 **B** ($\delta = 3.73$ ppm) with H-1 **F** ($\delta = 4.94$ ppm). Residue **A** was substituted at O-2 and O-6. Thus, the NOE correlation of H-6 **A** ($\delta = 4.09/3.71$ ppm) with H-1 **E** of α-Glc evidenced the substitution of residue **A** at O-6 by the α-glucose **E**. Furthermore the α-galactose was glycosylated at position O-2 by the α-heptose **D′**, as evidenced by the NOE contact of H-2 of **A** ($\delta = 3.69$ ppm) with H-1 of **D′** ($\delta = 5.07$ ppm). The HMBC spectrum confirmed the structure assigned so far, because it contained all of the required long-range correlations to demonstrate the proximity of the residues. Thus, the methylation analyses, glycosylation shifts and NOE data are all in agreement and indicate the oligosaccharide structure (oligosaccharide **X**) below:

F-(1→7)-**B**-(1→3)-**C**-(1→5)-**K**-(2→
3 4
↑ ↑
1 1
D'-(1→2) **A** **I**
6
↑
E

An alternative glycoform of the α-heptose **D′** was found, namely residue **D** (H-1 $\delta = 5.08$ ppm, see Figure 3 and Table 1), identified as a 7-α-Hep. The NOE contact of H-7 **D** with H-1 of the β-D-QuiN **H**, evidenced the glycosylation of the 7-position by residue **H**. Residue **H** was, in turn, substituted at O-3 by the terminal α-rhamnose **G**, as suggested by the NOE contact between H-1 of **G** and H-3 of **H**. The long-range scalar connectivity in the HMBC spectrum confirmed this oligosaccharide sequence. These data validated the following structure, differing from the above oligosaccharide **X** for the presence of the additional terminal disaccharide [**G-**(1→3)-**H-**(1→7)-(oligosaccharide **Y**):

F-(1→7)-**B**-(1→3)-**C**-(1→5)-**K**-(2→
3 4
↑ ↑
1 1
G-(1→3)-**H**-(1→7)-**D**-(1→2) **A** **I**
6
↑
E

The appearance of the anomeric signals of **A** and **E** as triplets (Figure 2) was most likely due to the heterogeneity determined by the non-stoichiometric presence of the terminal disaccharide [QuiNAc-(1→3)-Rha-(1→], which induces small shifts of the H-1 signals. The induced shift in the resonance of the residue of α-heptose, to which the disaccharide is linked, and which is also split into two signals, **D** and **D′** can be explained in the same way.

A MALDI mass spectrum of the oligosaccharide mixture **OS1** completely confirmed our structural hypotheses (Figure 4a). The negative-ion mass spectrum showed two major ions at $m/z = 1491.9$ and 1825.2 ($\Delta m/z = 333$). The species at $m/z = 1491.9$ was identified as the octasaccharide **X**, which is built up of four Hep, three Hex and one Kdo residues. The species at $m/z = 1825.2$ ($\Delta m/z = 333$) was consistent with the decasaccharide **Y**, which differs from **X** by the presence of the additional D-Hex–D-HexNAc disaccharide.

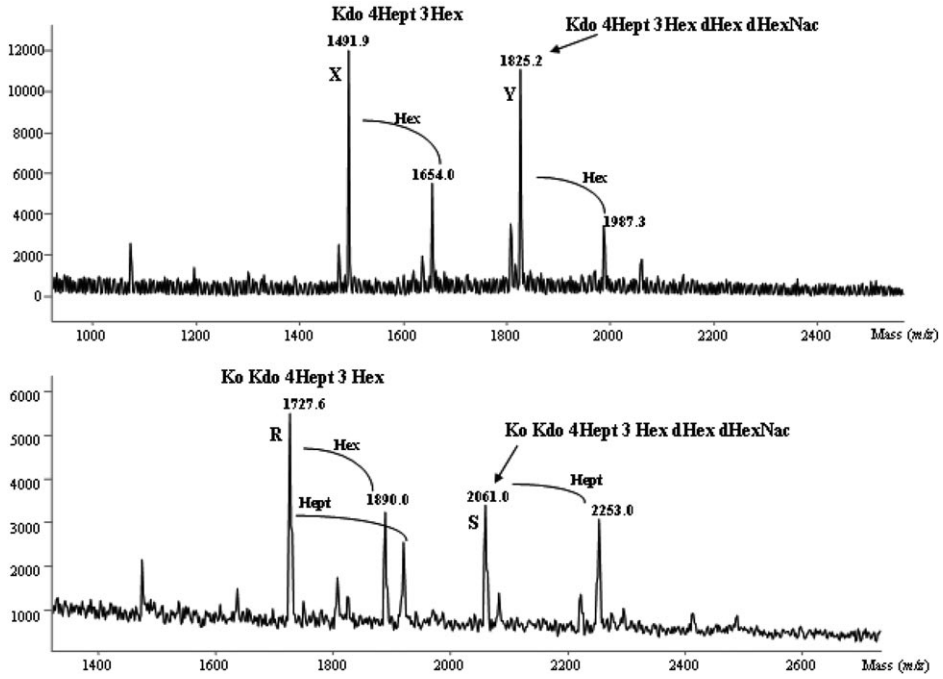

Figure 4. Top: Negative-ion MALDI mass spectrum of **OS1** product. Bottom: Negative-ion MALDI mass spectrum of **OS2** product.

The oligosaccharide species corresponding to the ions at $m/z = 1654.0$ and 1987.3 carried an adjunctive Hex residue with respect to oligosaccharide **X** and **Y**, and were not visible by NMR spectroscopy. The presence of a 6-substituted glucose (see above and Table S1 of the Supporting Information) indicated that this additional non-stoichiometric residue, when present, was located at O-6 of one of the two terminal hexoses of **OS1**, namely, residues **E** and **I**. In analogy to the core structure of other *Burkholderia* and *Pseudomonas* LPSs characterised thus far,[8,14] this glucose can be placed at O-6 of residues **I**.

MALDI-MS characterisation of the OS2 product: The second oligosaccharide fraction **OS2** isolated by means of gel-permeation chromatography underwent a mass spectrometric investigation. A methylation analyses revealed the presence of a 3,4-disubstituted Hep, a 3,7-disubstituted Hep, a 7-substituted Hep, a terminal Hep, a 2,6-disubstituted Gal, a 6-substituted Glc, a terminal Glc, a terminal Rha, a 3-substituted QuiN, a 4,5-substituted Kdo, a terminal Ko and a heptose disaccharide formed by Hep-(1→7)-Hep. A mild methanolysis treatment (0.5 M HCl/MeOH, 85 °C, 45 min) allowed the isolation of the disaccharide Ko-(2→4)-Kdo.

The negative-ion MALDI mass spectrum of the oligosaccharide mixture **OS2** showed several ion species that differed for the length of the sugar skeleton. The ion **R** (Figure 4b) at $m/z = 1727.6$ was built up of four Hep, three Hex, one Kdo and one Ko residue. Species **R** matched with species **X**, which was present in the oligosaccharide **OS1** (Figure 4b) with an additional Ko moiety. Species **S** at $m/z = 2061.0$ ($\Delta m/z = 333$ from **R**) was consistent with an undecasaccharide that differed by the presence of the additional dHex–dHexNAc disaccharide and matched with species **Y**, which was present in the oligosaccharide **OS1**, with an additional Ko moiety. Species carrying an additional Hep or Hex residue with respect to **R** and **S** were also present in the MALDI mass spectrum. The additional Hep was obviously linked at O-7 of the terminal heptose residue (residue **F** in **OS1**, see above), as demonstrated by the Hep-(1→7)-Hep disaccharide found by GC-MS analysis.

By merging the information deriving from **OS1** and **OS2**, it was possible to define a single oligosaccharide sequence:

α-L,D-Hep-(1→7)-α-L,D-Hep-(1→7)-α-L,D-Hep-(1→3)-α-L,D-Hep-(1→5)-α-D-Kdo-(4→2)-α-D-Ko
3 4
↑ ↑
1 1
β-D-QuiNAc-(1→7)-α-L,D-Hep-(1→2)-α-D-Gal β-D-Glc
3 6
↑ ↑
1 1
α-L-Rha α-D-Glc

At this stage it can be supposed that the glycosydic linkage of the Ko unit in **OS1** was most likely partially cleaved during the acid hydrolysis.

Structural characterization of the de-O-acylated LOS fraction: To characterise the saccharide backbone of the lipid A moiety, the LOS was de-O-acylated by mild hydrazinolysis, and the product (**OS3**) underwent a complete chemical and NMR investigation (see Supporting Information). On the basis of the NMR data, the phosphate substitution pattern can be summarized in this way: the α-GlcN of lipid A carries a phosphate group at an anomeric position that is not stoichiometrically substituted by a 4-deoxy-4-amino-arabinose moiety, and the β-GlcN always carries a phosphate group at position O-4.

Structural characterisation by MALDI mass spectrometry of the intact LOS and Lipid A: To confirm the structure of the lipid A core region, and to gain more information about the non-carbohydrate substituents, the intact LOS and the lipid A were analysed by MALDI MS. The negative-ion MALDI mass spectrum of intact LOS (Figure 5a,b) showed ion peaks related to fragments that arose from the very labile glycoside bond cleavage between Kdo and the lipid A moiety.[15] Molecular ions in the mass range 3000–4200 Da were also present. This fragmentation arises from a β-elimination and yields either an oligosaccharide ion (B-type ions) or a lipid A ion (Figure 5a). Thus, at low molecular masses (Figure 5a), the two ion peaks derived from the core oligosaccharide and were in accordance with the structure that we have deduced above. The ion peak **A** at $m/z=$ 1709.7 was the nonasaccharide carrying four heptoses, three hexoses, one Kdo and one Ko, whereas the ion **B** at $m/z=$ 2043.6 was the undecasaccharide carrying the adjunctive D-Hex–D-HexNAc disaccharide ($\Delta m/z=333.9$ from **A**). The two ions, **A** and **B** chemically matched the major oligosaccharide species **OS1** (that lacks the Ko residue) and **OS2**, previously characterised. In the same mass range, ion peaks deriving from the lipid A were identified. The lipid A was constituted by a mixture of tetra- and pentaacylated species differing by the phosphorylation pattern (species **I**–**IV**) (Figure 5a). Species **I** at $m/z=1444.7$ was consistent with a tetraacylated disaccharide backbone that carries a 14:0 (3-OH) chain in the ester linkage, and two 16:0 (3-OH) chains in the amide linkage, one of which, on the GlcN II, was further substituted by a secondary fatty acid residue, a 14:0 residue.

Species **II** at $m/z=1575.7$ ($\Delta m/z=131$) carried an additional Ara4N residue with respect to species **I**. Species **III** and **IV** were the corresponding pentaacylated species carry-

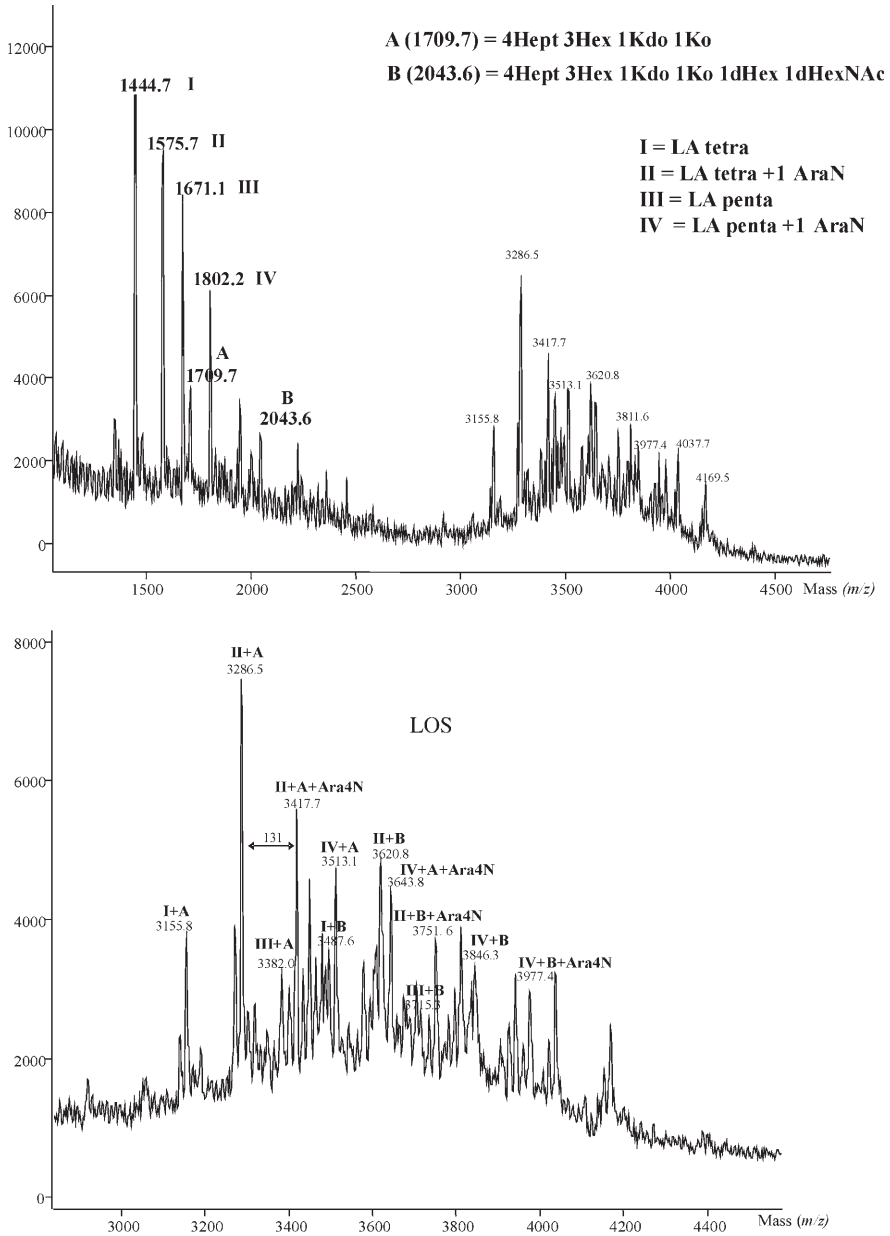

Figure 5. Top: Negative-ion MALDI TOF mass spectrum of intact LOS of *B. cenocepacia* obtained in linear mode. Bottom: High mass region of the same mass spectrum showing molecular ions.

ing two ester-linked 14:0 (3-OH) residues. The location of the secondary fatty acid 14:0 on the GlcN II was determined by the analysis of the lipid A, which was isolated as a precipitate by acetate buffer hydrolysis (see above). Thus, in the positive-ion MALDI mass spectrum, the triacylated oxonium ion at $m/z = 933.7$ (not shown), which arose from the glycosydic cleavage of the non-reducing GlcN unit, was ascribed to a triacylated oxonium ion carrying a 14:0 (3-OH), a 14:0 and a 16:0 (3-OH) residue. To assign the secondary fatty acid position, the LOS was hydrolysed with ammonium hydroxide,[16] and the product was analysed by MALDI MS (not shown). This approach resulted in the identification of the location of the amide-bound acyloxyacyl moiety, that was left unaltered by this mild hydrolysis. In fact, the spectrum that registered in negative-mode contained an ion peak at $m/z = 1218.8$, which was related to a triacylated bisphosphorylated lipid A species with two amide-linked 16:0 (3-OH) residues, one of which was substituted by a C14:0. Minor species at $m/z = 1444.5$ carried an additional ester-linked C14:0 (3-OH) residue ($\Delta m/z = +226$). Moreover, it was also possible to detect two other ions at $m/z = 1349.6$ and 1575.6, which were identified as tri- and tetraacylated lipid A species carrying an additional Ara4N residue.

The LOS molecular ions in the mass range 3000–4000 Da (Figure 5b) were given by the combination of the peaks of lipid A and the core region. Interestingly, the peaks related to the presence of an additional pentosamine that is located in the core region were also present (e.g., see the ion at $m/z = 3417.7$). This pentosamine was identified by GC-MS as Ara4N. This last residue was evidently linked at position O-8 of the Ko residue, as shown by the GC-MS analysis, which showed the existence of a Kdo–Ko–Ara4N trisaccharide, in accordance with prior data.[11,17–18]

In summary, the complete structure of the lipo-oligosaccharide (Figure 6) from the virulent strain of *B. cenocepacia* ET-12 LMG 16656 (strain J2315) has been carried out by chemical analyses, MALDI MS and 2D NMR spectroscopy.

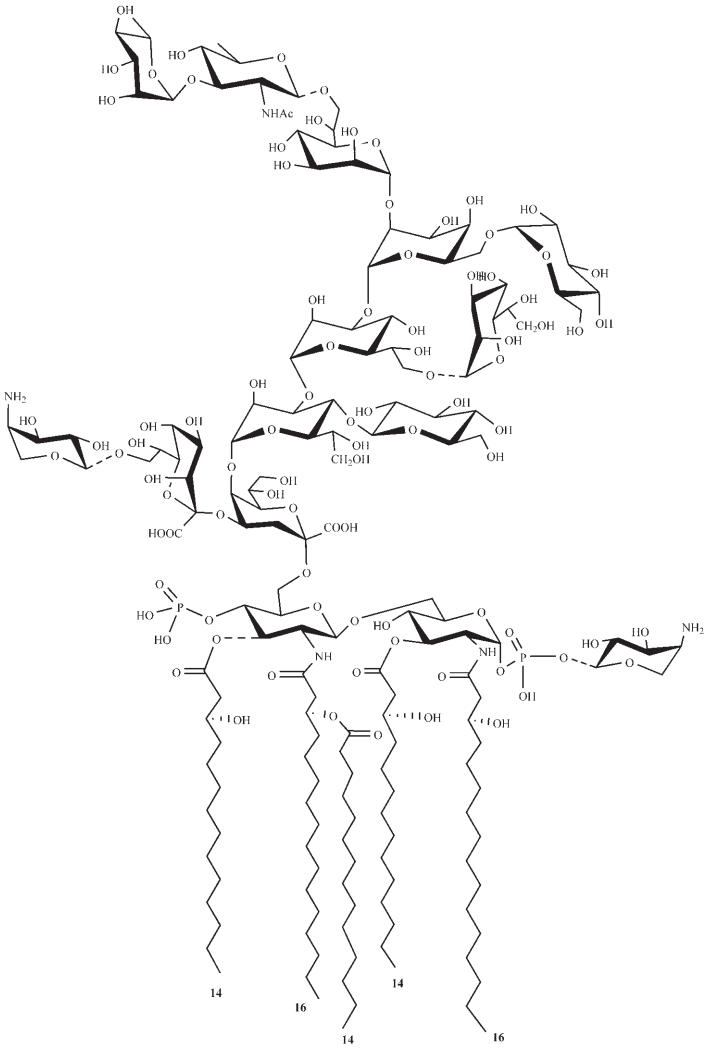

Figure 6. The structure of the lipooligosaccharide from *Burkholderia cenocepacia*. The dotted line indicates non-stoichiometric substitution.

Discussion

This is the first report on the primary structure of the R-LPS from LMG 16656, the ET-12 clone type strain of *B. cenocepacia* (also known as J2315), perhaps the most notorious and feared single strain in cystic fibrosis. The ability of this LOS to induce TNF-α production in a U937 macrophage reporter assay is also described.

Although other epidemic strains may prevail depending on geographical location, the *B. cenocepacia* ET-12 clone has been responsible for epidemics in CF centres in the UK and Canada, and is one of the most common strains in CF patients noted worldwide.[19–21] Upon infection, this strain is also associated with increased morbidity and mortality in CF patients, and has been associated with high mortality rates following lung transplantation in CF recipients with preoperative ET-12 infections.[22] Infection with any of the *B. cepacia* complex may be characterised by accelerated lung disease in some patients with pre-existing mild to moderate lung disease. Overwhelming septicaemia and necrotising pneumonia most commonly due to *B. cenocepacia*, "the cepacia syndrome" are well-described events, but are extremely rare with other potentially pathogenic bacteria such as *P. aeruginosa*.

The hallmark of BCC infection in CF is the inflammation that results from the peculiar biochemical properties of lipopolysaccharide, which is able to induce the local release of pro-inflammatory factors and, in turn, induce host defence responses and tissue damage. An important component of the immune response is the production of cationic peptides that act as antimicrobial molecules by damaging the bacterial membrane through electrostatic interactions.[3,9–10] Lipid A is recognized as the endotoxin portion of the LPS, and is responsible for the strong immunostimulatory activity. Recently, in a very interesting paper, it has been demonstrated that it is necessary for *B. cenocepacia* to possess the complete core oligosaccharide attached to lipid A for it to maintain its

resistance to antimicrobial peptides, and for in-host survival.[23] In fact, a mutant expressing defective heptosyl transferase, and therefore unable to carry out the biosynthesis of the whole LPS was found to be sensitive to mellitine and polymyxin B. In contrast, a mutant strain that produced a complete core-oligosaccharide–lipid A skeleton, but lacked the O-antigen, was not sensitive to cationic peptides. In the same paper, it has also been shown that the core oligosaccharide is necessary for the in vivo survival of the bacterium in a rat model of chronic lung infection.

Despite the wealth of significant biological data on *B. cenocepacia*, and on an ET-12 wild-type strain in particular, only partial data regarding the structure of the LPS from *B. cenocepacia* were known.[5] We have therefore addressed the structural elucidation of the whole molecule and, on this ground, some further considerations can be made.

From the chemical point of view, in accordance with all of the other lipopolysaccharides from the *Burkholderia* genus that have been elucidated so far, even in the *B. cenocepacia* LOS no negative charges are present in the outer core, which contains neither uronic acids nor phosphate groups. The lipid A moiety possesses a carbohydrate backbone that is characterised by a P→4-β-D-Glc*p*N-(1→6)-α-D-Glc*p*N-(1→P)-Ara4N sequence. The lipid A is further glycosylated by a Kdo unit that is in turn substituted at O-5 with a Ko residue. The latter bears a second Ara4N residue. The Ara4N–Ko–Kdo trisaccharide sequence, previously reported in other *Burkholderia* species,[11,17–18] seems unique and distinctive of *Burkholderia* LPSs. The Ko monosaccharide is also limited to a few bacterial LPS molecules, like *Acinetobacter*,[24] *Yersinia*[25] and *Serratia*,[26] in particular, but only in *Acinetobacter* LPS is Ko directly linked to the lipid A backbone and is not a substituent of the first Kdo residue.[24] The lipid A inner core region is a key element in the provirulent strategy of *B. cenocepacia* (and of BCC species in general), which consists of covalent modifications, such as the addition of Ara4N, in order to reduce the surface net charge, and in turn to reduce the ionic attraction for cationic antimicrobial peptides. However, it is clear that this is not the only mechanism by which *B. cenocepacia* eludes the immune response. In fact, the presence of the complete core oligosaccharide is mandatory in the LOS for the survival of the bacterium.[23] Moreover, the presence in the outer core region of a non-stoichiometric amount of a Rha-QuiNAc disaccharide suggests that the disaccharide is preassembled before transfer to the terminal position. The role of this disaccharide is unknown, although it may be speculated that it could function as a cap, precluding the linkage of the O-chain to the core oligosaccharide. Interestingly, this disaccharide moiety is held by a heptose residue that is infrequently found as a component of the outer core of LOSs.[8] Its presence implicates the existence of an additional, different heptosyl transferase.

From a biochemical point of view, the greater clinical and pro-inflammatory impact of *B. cenocepacia* as compared to other BCC species can be partially ascribed to the structural differences on the lipid A inner core region, for example, the amount of Ara4N residues and a slightly different acylation pattern. From a comparion of previously published data on lipid A from *B. cepacia* genomovar I,[18] *B. multivorans* and *B. cenocepacia*[5], it appears that there are many lipid A species that are shared between genomovars, which suggests a common lipid A biosynthesis pathways. The predominant production of a specific lipid A moiety by a genomovar could be induced by environmental stimuli, or it could reflect the preferential lipid A biosynthesis, which may confer an evolutionary advantage for the organism. Most of the strains studied so far express a variety of lipid A species. In general, the more highly acylated lipid A is, the greater the immune system activation and cytokine induction that is evoked. *B. cenocepacia* expresses high levels of pentaacyl lipid A, the highest possible acylation pattern for its LPS, and this may contribute to the significant immunological response observed in this study. Importantly, amongst all of the LPS/LOS that were isolated from ET-12 clones and tested in our tissue culture system, there appeared to be a variety of biological activity with LMG 12614 and LMG 16656, which elicited more TNF-α than LMG 18863 (also known as strain K56-2). This could explain in part why there can be variable outcomes between patients who are apparently infected with the same clonal strain. Whilst there is a temptation to assume that all ET-12 clones behave similarly in experimental models, our data suggests that there is diversity even amongst a panel of closely related ET-12 clones. There was variable cytokine induction capacity in the ET-12 clones tested; LMG 12614 and LMG 16656 (J2315) were potent TNF-α inducers, whilst LMG 18863 (K56–2) and the *B. multivorans* strain LMG 14273 were relatively poor inducers. Moreover, prior data reported that strain LMG 16656 induced a ninefold higher release of cytokines than *Pseudomonas aeruginosa* LPS.[27]

The structure of this particular ET-12 clone has been of great importance given the recent completion of the sequencing project at the Sanger Centre using this specific strain. In fact, it has long been recognized that there is subclonal variation between ET-12 clones, and any attempts at genetic manipulation of the lipid A biosynthesis and virulence down-regulation will depend upon knowing both the structure and the genetic basis of such biosynthesis pathways. Furthermore, the knowledge of such virulence factors is crucial for the comprehension of the molecular mechanisms of BCC infections, that is, to what extent LPS is an important factor for initiating or manipulating immune activation in the early phase of infection.

We believe that this is a first step toward the design of antimicrobial compounds and for the development of therapeutic strategies against the inflammatory cascade.

Experimental Section

Bacterial growth and LPS extraction: Strain LMG 16656 (*B. cenocepacia* ET-12 type strain), LMG 12614, LMG 18863 (additional ET-12 clones) and LMG 14273 *B. multivorans* strain were obtained from the Belgium

Coordinate Collection for Microbes and grown as described.[5] The LPS extraction was carried according to a published method.[28] The LPS fractions were analyzed by SDS-polyacrylamide gel electrophoresis on 16% gels, which were stained with silver nitrate.[14]

Cell stimulation assays: Human myelomonocytic U937 cells were prepared as described.[5]

Detection of cytokine induction: This assay was carried out by using ELISA on the supernatants of stimulated U937 cells. The assays for Tumour Necrosis Factor-alpha (TNF-α, Pharmingen, UK) were performed by using paired antibodies as described previously.[5] Statistical testing was undertaken using a T-test.

Isolation of oligosaccharide OS1, OS2 and OS3: The lipid A and the core oligosaccharide (**OS1** (1 mg) and **OS2** (0.5 mg)) were isolated as described previously.[31] An aliquot of LOS (5 mg) was de-O-acylated as previously described (**OS3** 3.5 mg). [29]

General and analytical methods: The determination of sugars residues, of their absolute configuration and linkage analysis, of total fatty acids content and of their absolute configuration were all carried out as previously described.[30–34]

NMR spectroscopy: For structural assignments of **OS1** and **OS2**, 1D and 2D ^{1}H NMR spectra were recorded in 0.5 mL of D_2O at 300 K, pD 7 (uncorrected value) on Bruker 600 DRX equipped with a cryo probe. For structural assignments of **OS3**, 1D and 2D ^{1}H NMR spectra were recorded in a solution of 1% deuterated SDS (sodium dodecyl sulphate) with 5 μL of 32% NH_4OH at 298 K, pD 9.5 (uncorrected value). Spectra were calibrated with internal acetone ($\delta_H = 2.225$ ppm, $\delta_C = 31.45$ ppm). ^{31}P NMR experiments were carried out using a Bruker DRX-400 spectrometer, aqueous 85% phosphoric acid was used as an external reference ($\delta = 0.00$ ppm). Rotating frame Overhauser enhancement spectroscopy (ROESY), total correlation spectroscopy (TOCSY), double quantum-filtered phase-sensitive correlation spectroscopy (DQF-COSY), heteronuclear single quantum coherence (HSQC) and heteronuclear multiple bond correlation (HMBC) experiments were performed and processed as described.[29] Coupling constants were determined on a first-order basis from DQF-COSY.[35–36] Experiments were carried out in the phase-sensitive mode according to the method of States et al.[37]

MALDI TOF mass spectrometry: MALDI-TOF mass spectra were recorded in the negative and positive polarity in linear-mode on a Perseptive (Framingham, MA, USA) Voyager STR equipped with delayed extraction technology. Ions formed by a pulsed UV laser beam (nitrogen laser, $\lambda = 337$ nm) were accelerated by 24 kV. The mass spectra reported are the result of 256 laser shots. The resolution was about 1500.

OS, LOS and lipid A sample preparation: The oligosaccharide mixture was analyzed as described.[38] Recrystallization from methanol was performed as reported.[39] The R-type LPS was prepared as recently reported.[15] The MALDI preparation of lipid A samples was performed as described.[40]

Acknowledgements

The 600 MHz cryoprobe NMR facilities were provided by the spectrometer of the Centro Regionale di Competenza in Biotecnologie Industriali BioTekNet. M.P. is grateful for the financial support of MIUR-Roma (Progetto di Ricerca di Interesse Nazionale, 2004, Roma). We also thank the Special Trustees of the Newcastle Hospitals.

[1] L. Eberl, *Int. J. Med. Microbiol.* **2006**, *296*, 103–110.
[2] E. Yabuuchi, Y. Kosako, H. Oyaizu, I. Yano, H. Hotta, Y. Hashimoto, T. Ezaki, M. Arakawa, *Microbiol. Immunol.* **1992**, *36*, 1251–1275.
[3] E. Mahenthiralingam, T. A. Urban, J. B. Goldberg, *Nat. Rev. Microbiol.* **2005**, *3*, 144–156.
[4] L. Chiarini, A. Bevivino, C. Dalmastri, S. Tabacchioni, P. Visca, *Trends Microbiol.* **2006**, *14*, 277–286.
[5] A. De Soyza, C. D. Ellis, C. M. A. Khan, P. A. Corris, R. Demarco de Hormaeche, *Am. J. Respir. Crit. Care Med.* **2004**, *170*, 70–77.
[6] R. M. Aris, J. C. Routh, J. J. Lipuma, D. G. Heath, P. H. Gilligan, *Am. J. Respir. Crit. Care Med.* **2001**, *164*, 2102–2106.
[7] G. Seltmann, O. Holst, *The Bacterial Cell Wall*, Springer, Heidelberg, **2001**.
[8] O. Holst in *Endotoxin in Health and Disease* (Eds: H. Brade, D. C. Morrsion, S. Opal, S. Vogel), Dekker, New York, **1999**, pp. 115–154.
[9] C. R. H. Raetz, C. Whitfield, *Annu. Rev. Biochem.* **2002**, *71*, 635–700.
[10] C. Alexander, E. T. Rietschel, *J. Endotoxin Res.* **2001**, *7*, 167–202.
[11] Y. Isshiki, K. Kawahara, U. Zähringer, *Carbohydr. Res.* **1998**, *313*, 21–27.
[12] G. I. Birnbaum, R. Roy, J. R. Brisson, H. Jennings, *J. Carbohydr. Chem.* **1987**, *6*, 17–39.
[13] O. Holst, J. E. Thomas-Oates, H. Brade, *Eur. J. Biochem.* **1994**, *222*, 183–194.
[14] R. Kittelberger, F. Hilbink, *J. Biochem. Biophys. Methods* **1993**, *26*, 81–86.
[15] L. Sturiale, D. Garozzo, A. Silipo, R. Lanzetta, M. Parrilli, A. Molinaro, *Rapid Commun. Mass Spectrom.* **2005**, *19*, 1829–1834.
[16] A. Silipo, R. Lanzetta, A. Amoresano, M. Parrilli, A. Molinaro, *J. Lipid Res.* **2002**, *43*, 2188–2195.
[17] S. Gronow, C. Noah, A. Blumenthal, B. Lindner, H. Brade, *J. Biol. Chem.* **2003**, *278*, 1647–1655.
[18] A. Silipo, A. Molinaro, D. Comegna, L. Sturiale, P. Cescutti, D. Garozzo, R. Lanzetta, M. Parrilli, *Eur. J. Org. Chem.* **2006**, 4874–4833.
[19] J. R. Govan, P. H. Brown, J. Maddison, C. J. Doherty, J. W. Nelson, M. Dodd, A. P. Greening, A. K. Webb, *Lancet* **1993**, *342*, 15–19.
[20] A. De Soyza, A. McDowell, L. Archer, J. H. Dark, S. J. Elborn, E. Mahenthiralingam, K. Gould, P. A. Corris, *Thorax* **2004**, *59*, 526–528.
[21] G. Golini, G. Cazzola, R. Fontana, *Eur. J. Clin. Microbiol. Infect. Dis.* **2006**, *25*, 175–180.
[22] A. De Soyza, A. McDowell, L. Archer, J. H. Dark, S. J. Elborn, E. Mahenthiralingam, K. Gould, P. A. Corris, *Lancet* **2001**, *358*, 780–781.
[23] S. A. Loutet, R. S. Flannagan, C. Kooi, P. A. Sokol, M. A. Valvano, *J. Bacteriol.* **2006**, *188*, 2073–2080.
[24] E. V. Vinogradov, S. Müller-Loennies, B. O. Petersen, S. Meshkov, J. E. Thomas-Oates, O. Holst, H. Brade, *Eur. J. Biochem.* **1997**, *247*, 82–90.
[25] E. V. Vinogradov, B. Lindner, N. A. Kocharova, S. N. Senchenkova, A. S. Shashkov, Y. A. Knirel, O. Holst, T. A. Gremyakova, R. Z. Shaikhutdinova, A. P. Anisimov, *Carbohydr. Res.* **2002**, *337*, 775–777.
[26] E. V. Vinogradov, B. Lindner, G. Seltmann, J. Radziejewska-Lebrecht, O. Holst, *Chem. Eur. J.* **2006**, *12*, 6692–6700.
[27] D. Shaw, I. R. Poxton, J. R. Govan, *FEMS Immunol. Med. Microbiol.* **1995**, *11*, 99–106.
[28] O. Westphal, K. Jann, *Methods Carbohydr. Chem.* **1965**, *5*, 83–91.
[29] A. Silipo, A. Molinaro, L. Sturiale, J. M. Dow, Erbs G. R. Lanzetta, M. A. Newman, M. Parrilli, *J. Biol. Chem.* **2005**, *280*, 33660–33668.
[30] K. Leontein, J. Lönngren, *Methods Carbohydr. Chem.* **1978**, *62*, 359–362.
[31] A. Molinaro, C. De Castro, R. Lanzetta, A. Evidente, M. Parrilli, O. Holst, *J. Biol. Chem.* **2002**, *277*, 10058–10063.
[32] S. Hakomori, *J. Biochem.* **1964**, *55*, 205–208.
[33] A. Silipo, R. Lanzetta, D. Garozzo, P. L. Cantore, N. S. Iacobellis, A. Molinaro, M. Parrilli, A. Evidente, *Eur. J. Biochem.* **2002**, *269*, 2498–2505.
[34] E. T. Rietschel, *Eur. J. Biochem.* **1976**, *64*, 423–428.
[35] U. Piantini, O. W. Sørensen, R. R. Ernst, *J. Am. Chem. Soc.* **1982**, *104*, 6800–6801.
[36] M. Rance, O. W. Sørensen, G. Bodenhausen, G. Wagner, R. R. Ernst, K. Wüthrich, *Biochem. Biophys. Res. Commun.* **1983**, *117*, 479–485.
[37] D. J. States, R. A. Haberkorn, D. J. Ruben, *J. Magn. Reson.* **1982**, *48*, 286–292.

[38] A. Silipo, A. Molinaro, E. L. Nazarenko, L. Sturiale, D. Garozzo, R. P. Gorshkova, O. I. Nedashkovskaya, R. Lanzetta, M. Parrilli, *Carbohydr. Res.* **2005**, *340*, 2540–2549.

[39] E. Spina, R. Cozzolino, E. Ryan, D. Garozzo, *J. Mass Spectrom.* **2000**, *35*, 1042–1048.

[40] A. Silipo, L. Sturiale, D. Garozzo, C. de Castro, R. Lanzetta, M. Parrilli, W. Grant, A. Molinaro, *Eur. J. Org. Chem.* **2004**, 2263–2271.

Received: October 2, 2006
Published online: January 12, 2007

